ALMA MATER STUDIORUM - UNIVERSITÀ DI BOLOGNA

CAMPUS DI CESENA

DIPARTIMENTO DI

INGEGNERIA DELL'ENERGIA ELETTRICA E DELL'INFORMAZIONE

"GUGLIELMO MARCONI"

CORSO DI LAUREA IN INGEGNERIA BIOMEDICA

EVALUATION OF THE SIZE AND DENSITY OF OSTEOCYTE LACUNAE IN METASTATIC BONE CORES

Elaborato in

Comportamento Meccanico Dei Biomateriali E Delle Strutture (c.i.)

Relatore

Prof. Marco Palanca

Presentata da

Elena Roncassaglia

Correlatore

Ing. Giulia Cavazzoni

Dr. Enrico Dall'Ara

Anno Accademico 2022/23

Abstract

L'osso è uno dei siti più comuni in cui le metastasi proliferano: esse contribuiscono all'alterazione della meccano-sensazione e della meccano-trasduzione regolate dagli osteociti, il tipo di cellula più abbondante nell'osso. Indagare gli effetti delle metastasi a livello microstrutturale e comprendere la relazione tra la dimensione e la distribuzione delle lacune osteocitarie nei nuclei ossei estratti da ossa con metastasi può essere utile per comprendere il loro ruolo nella formazione e nello sviluppo del tessuto blastico.

Lo scopo di questo studio era di valutare la dimensione e la distribuzione delle lacune degli osteociti nei nuclei estratti da ossa con metastasi.

Nove nuclei ossei sono stati estratti da vertebre lombari affette da metastasi blastiche e scansionate con micro-TC per indagare a livello microstrutturale le proprietà microstrutturali e le proprietà delle lacune osteocitarie. I risultati ottenuti dall'analisi microstrutturale hanno mostrato che lo spessore trabecolare (Tb.Th) e la separazione trabecolare (Tb.Sp) sono risultati inferiori in questo studio rispetto agli studi basati su nuclei ossei umani sani. Allo stesso modo, il numero di lacune (N.Lc) è risultato inferiore in questo studio rispetto agli studi basati su nuclei ossei corticali estratti da ossa umane sane. Inoltre, il volume totale delle lacune (Lc.TV) e la densità del numero di lacune (N.Lc/TV) sono risultati più elevati in questo studio rispetto ad altri studi con valori simili di numero di lacune ma con ossa umane sane. Questi risultati indicano che, poiché gli osteociti, che sono responsabili della meccanotrasduzione e della meccanosensazione, sono formati a partire da osteoblasti che creano nuovo tessuto osseo, le lacune osteocitarie potrebbero avere un ruolo fondamentale nello sviluppo delle metastasi.

In conclusione, i risultati di questo studio evidenziano l'importanza di indagare i parametri microstrutturali delle lacune degli osteociti nei nuclei ossei estratti dalle vertebre con tessuto blastico per comprendere il loro ruolo nella formazione e nello sviluppo del tessuto blastico.

Abstract

Bone is one of the most common sites of metastases, which contribute to the alteration of mechano-sensation and mechano-transduction regulated by osteocytes, the most abundant cell type in bone. Investigating the effects of metastases at the microstructural level and understanding the relationship between the dimension and distribution of osteocyte lacunae in bone cores extracted from bones with metastases can be useful to understand their role in the formation and development of blastic tissue.

The aim of this study was to evaluate the size and distribution of osteocyte lacunae in cores extracted from bone with metastases.

Nine bone cores were extracted from lumbar vertebrae affected by blastic metastases and micro-CT scanned to investigate at microstructural level the microstructural properties and the properties of the osteocyte lacunae. The results obtained from the microstructural analysis showed that trabecular thickness (Tb.Th) an trabecular separation (Tb.Sp) resulted to be lower in this study when compared to studies based on healthy human bone cores. Similarly, the number of lacunae (N.Lc) resulted to be lower in this study when compared to studies based on cortical bone cores extracted from healthy human bones. Moreover, the total volume of lacunae (Lc.TV) and the density number of lacunae (N.Lc/TV) resulted to be higher in this study compared to other studies with similar values of number of lacunae but with healthy human bones. These results indicate that, since osteocytes, which are responsible for mechanotransduction and mechanosensation, are formed from osteoblasts which create new bone tissue, osteocytes lacunae could have a fundamental role in the development of metastases.

In conclusion, the outcomes of this study highlight the importance of investigating microstructural parameters of osteocytes lacunae in bone cores extracted from vertebrae with blastic tissue to understand their role in the formation and development of blastic tissue.

Contents

1. Introduction

1.1 Bone tissue

Bone tissue is a mineralized connective tissue that forms bones [1].

Two types of bone tissue exist: cortical bone and trabecular bone [2]. Cortical bone consists of osteons, the structural units of cortical bone: each osteon is formed by concentric bone lamellae. Each lamella is formed by parallel collagen fibers which are arranged concentrically. Trabecular bone is located in the internal part of the bone where the trabecular are arranged irregularly in order to create cavities among them. Cortical bone makes up about 80% of the total mass of bone and it is more abundant in long bones, while trabecular bone is about 20% of the total mass of bone and it is more abundant in flat and short bones, like vertebrae [2].

The bone tissue is composed of four types of cells (Fig.1): osteoblasts, osteoclasts, osteocytes, and bone lining cells [3]. Both osteoblasts and osteoclasts derive from mesenchymal stem cells. In particular, the osteoblasts are mononucleated cells which originate from the differentiation of osteoprogenitor cells, while osteoclasts are polynucleated cells that originate from preosteoclast. The main function of the osteoblasts is to synthesize the components that form the extracellular matrix of bone, such as collagen type I which constitutes the 90% of the extracellular matrix. Furthermore, osteoblasts support mineralisation of the extracellular matrix through matrix vesicles and extracellular organelles related to the matrix calcification.

The osteoclasts instead are involved in bone resorption which is essential for remodelling, growth, and repair of bone [3]. They migrate to the specific skeletal site where bone remodelling takes place.

Osteocytes are the most abundant cell type in bone, about 90%-95% of total bone cells. They are differentiated cells derived from osteoblasts. Osteocytes are localized in lacunae contained in the calcified bone matrix [4]. When the osteoid matrix is mineralized, osteoblasts get integrated into the mineral phase and transform themselves into

osteocytes. Thus, the osteocyte body is localized in the mineral lacuna, and is surrounded by bone fluid [5]. In order to preserve the viability of osteocytes, nutrients and waste products are transferred through long channels, called canaliculi [6]. The most important osteocyte's function is the regulation of bone mechanosensation and mechanotransduction [4]. Moreover, they are the master regulator of bone homeostasis through their regulation of calcium abundance during the mineralisation process. They also indirectly orchestrate the osteoblasts and osteoclasts activities.

Bone-lining cells are quiescent, flattened, and elongated osteoblasts that cover bone surfaces, where neither bone resorption nor bone formation occurs [4]. These cells prevent the interaction between osteoclasts and bone matrix when bone resorption should not occur, and they also take part in osteoclasts differentiation.

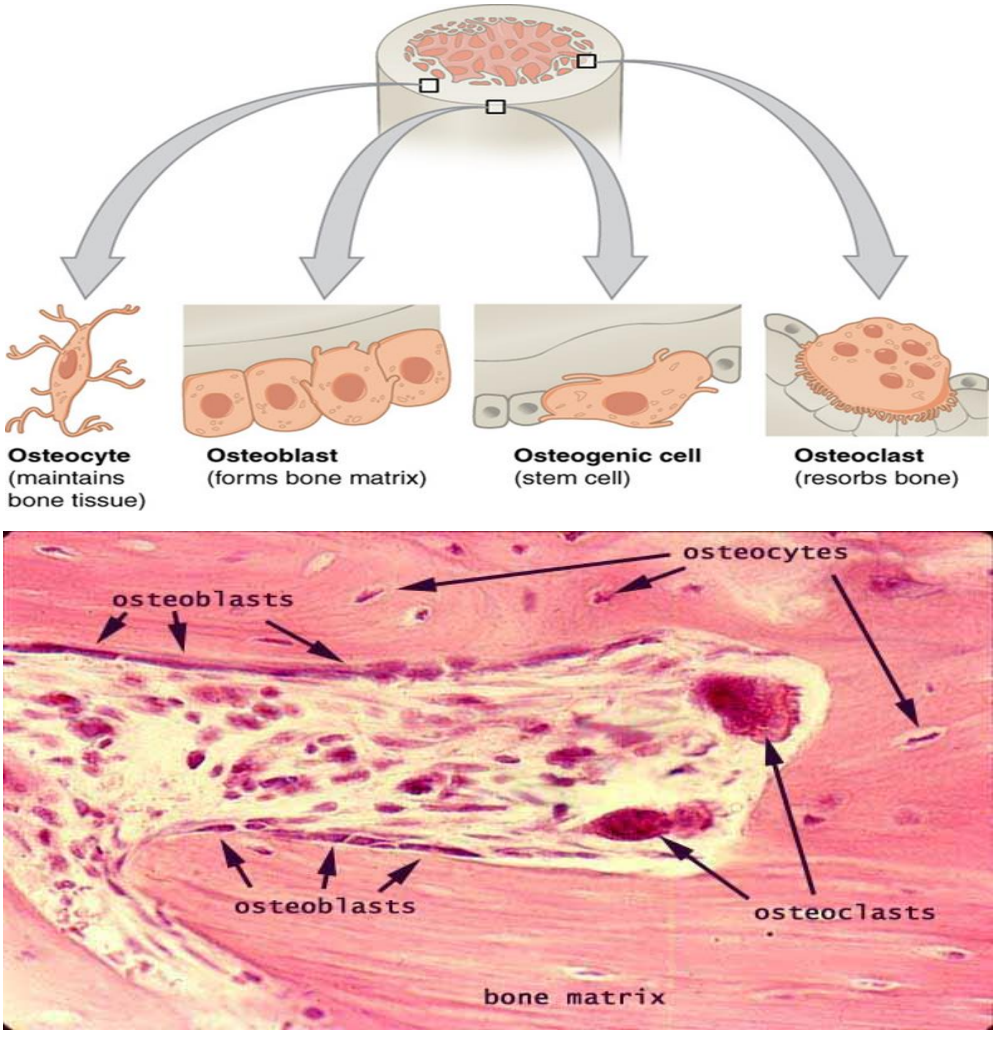

Figure 1: bone cells [7], [8].

1.2. Bone remodelling

Bone remodelling process is based on the activity of osteoblasts and osteoclasts that deposit new bone matrix and erode older bone tissue, respectively [9]. Bone formation and resorption are balanced in a homeostatic equilibrium: old bone is continuously replaced by new bone tissue.

Eriksen *et al* [10] hypothesized that bone remodelling mechanisms were different in case of trabecular and cortical bone tissue. In fact, the remodelling sites in trabecular bone are close to the red marrow, known to contain osteoprogenitor cells, the remodelling sites in cortical bone are distant from the red marrow. Cells required for bone remodelling in trabecular bone move from red marrow to bone surfaces, while cells reach cortical remodelling sites via the vasculature [11].

In both cases, bone remodelling takes place in the Basic Multicellular Unit (BMU) which includes osteoblasts, osteoclasts, and osteocytes in the bone-remodelling cavity [11]. The remodelling process consists of three consecutive phases: resorption, reversal, and formation. Resorption begins with the migration of preosteoclasts to the bone surface where they form osteoclasts. Then, during the reversal phase, mononuclear cells appear on the bone surface to prepare it for osteoblasts to begin bone formation and produce signals for osteoblasts migration and differentiation. Then, bone formation begins when osteoblasts start depositing new bone until the resorbed one is replaced. Finally, the surface is covered with bone-lining cells and a resting period begins until a new remodelling process [12].

It has been demonstrated that mechanical stress on bone tissue influences the remodelling process by stimulating formation and reducing resorption [13]. For decades osteoblasts were considered responsible for bone remodelling while osteocytes were inactive cells residing in the bone matrix [14]. However, some recent studies [15], [16] showed that osteocytes are those cells responsible for bone remodelling. Indeed, the mechanotransduction, i.e. the conversion of mechanical stimuli, is controlled by osteocytes [15], which regulate through cell signalling, the coordinated activity of osteoblasts and osteoclasts [14]. The main actor for bone remodelling from mechanical

stimulation seems to be the lacunae-canaliculi network: it is distributed throughout cortical bone and it is occupied by osteocytes surrounded by interstitial fluid [15]. Mechanical loading causes pressure changes in the fluid surrounding the osteocytes resulting in shear stresses applied to the osteocytes, that are sensed through the cytoskeleton of these cells [14], [15]. Once the stress is perceived by the osteocyte, cell signalling is activated to inhibit osteoclast bone resorption or promote osteoblast bone formation [16].

1.3 Bone remodelling in case of bone metastases

Metastases are secondary tumours which occur when cancer cells move from their original site, where the primary tumour is located, to another organ. Bone is one of the most common sites of metastases [17]: in fact there is a high blood flow around the region where red marrow is and cells release substances that cause faster cancer growth [18], [19]. Bone metastases are a frequent complication of cancer, occurring in up to 70% of patients with advanced breast or prostate cancer and in approximately 15% to 30% of patients with carcinoma of the lung, colon, stomach, bladder, uterus, rectum, thyroid, or kidney [20].

Tumours metastasize to bone produce numerous alterations in bone cell functionality, such as osteolysis[1] [21], osteopenia[2] [22], or anemia[3] [23]: in fact bone provides a fertile microenvironment that can support their growth by releasing cytokines as the bone matrix is destroyed [18]. Cancer cells release substances to stimulate osteoblasts or osteoclasts activity, which release growth factors that lead to vicious process of bone destruction and growth of the tumor [24].

Bone metastases are classified as osteoblastic, osteolytic or mixed (it has both osteolytic and osteoblastic components) according to their radiographic appearance [19]. In case of

[1] Progressive destruction of bone substance.

[2] Reduction of bone mineral density values.

[3] Hemoglobin deficiency in the blood.

osteoblastic metastases, regular process of bone homeostasis is compromised as the osteoblasts activity exceeds the bone resorption by the osteoclasts. By contrast, in case of osteolytic metastases, the process of bone resorption exceeds the activity of osteoblasts, resulting in bone degradation [19].

Metastatic lesions affect the bone quantity, quality, and architecture [25]: this condition causes changes of the dimension in the microporosity structure of the bone, of the lacuna-canalicular and vascular canals of the osteocytes. This contributes to the alteration of mechano-sensation and mechano-transduction regulated by osteocytes [25].

1.4 *Characterization of osteocytes in bone with metastases*

Osteocytes have been already partially studied from both a biological and mechanical point of view: their role has yet to be established in tumor biology.

1.4.1 Biological studies

In a recent study by Cui *et al* [24] it was evaluated the effect of Murine long bone osteocytes Y4 (MLO-Y4) cells on the proliferation, migration and invasion of breast and prostate cancer cells, which are the main types of tumours that metastasize to the bone. Osteocytes determine osteoclasts formation and control their activity by releasing factors, such as RANKL, that promote the differentiation of monocytes into osteoclasts which resorb bone. Furthermore, mechanical load increased the production of substances by osteocytes that facilitate the proliferation of osteoblasts in inflammatory conditions, as in the case of bone metastases. For these reasons, osteocytes are highly involved in the regulation of bone homeostasis.

In an early stage of the study, MLO-Y4 cells were treated with methotrexate, a substance used during chemotherapy: the treatment causes increase in the number of apoptotic osteocytes. Apoptotic osteocytes initiate targeted bone resorption by recruiting osteoclasts causing loss of bone homeostasis *in vivo*. Apoptosis also causes increased secretion of IL6 which enhances adhesion of osteoclast precursor to endothelial cells: IL6 is a mediator of

inflammatory cytokins which promotes proliferation and survival of tumour cells. However, it did not affect the proliferation of all tumour cells and therefore maybe the stimulation of proliferation by osteocytes depends on the type of tumour cell. According to the results, treating breast and prostate cancer lines with MLO-Y4, caused an increase of proliferation in all four tumour lines (two prostate cancer cell lines, namely DU145 and PC3, and two breast cancer cell lines, namely MDA-MB-231 and MCF-7), while it stimulated the migration of prostate cancer cells but inhibited the migration of breast cancer cells.

Another study by Sottnik *et al* [25] confirmed that the presence of metastases in the bone the presence of metastases increases the promotion of prostate cancer bone metastases growth by osteocytes. Prostate cancer cells were injected into the tibia of a mouse and intramedullary pressure caused by tumour growth was measured in vivo: in Cui study [24], osteocytes increased both proliferation and invasion of tumour cells. Tumours that produced mixed or osteoblastic lesions increase intramedullary pressure, increasing the secretion by osteocytes of factors that promote tumour cell proliferation. On the other hand, tumours that produced lytic lesions do not increase intramedullary pressure because osteolysis produce sufficient space for tumour development [26].

1.4.2 Microstructural studies

Different types of imaging techniques have been used to study bone microstructure and osteocyte lacunae: Standard micro-CT, X-ray nano-CT, Confocal Laser Scanning Microscopy (CLSM) and Synchrotron X-Ray Micro-CT.

Hemmanantian et al. [27] evaluated some microstructural features of lacunae in cortical bone of murine tibiae (lacuna volume, lacuna orientation, lacuna sphericity, lacuna volume density and lacuna number density), before and after the tumour cell line (breast EO771-Luc and prostate RM1-Luc) injection, using microcomputed tomography (micro-CT) with a resolution of 10 μm. were analysed. Breast (Fig.2A) and prostate (Fig.2D) cancer increased the lacunae volume by 12% and 10%, respectively. Besides, the number

of smaller lacunae (up to 200 μm3) was lower after the tumour cell line injection, whereas the number of larger lacunae (larger than 200 μm3) was elevated after the tumour cell line injection (Fig.B-E). Furthermore, in tibiae with breast cancer cells, osteocyte lacuna volume density was significantly higher in comparison to the control group, while mean lacuna orientation and sphericity were unaffected after cancer cells injection (Fig.2C-F).

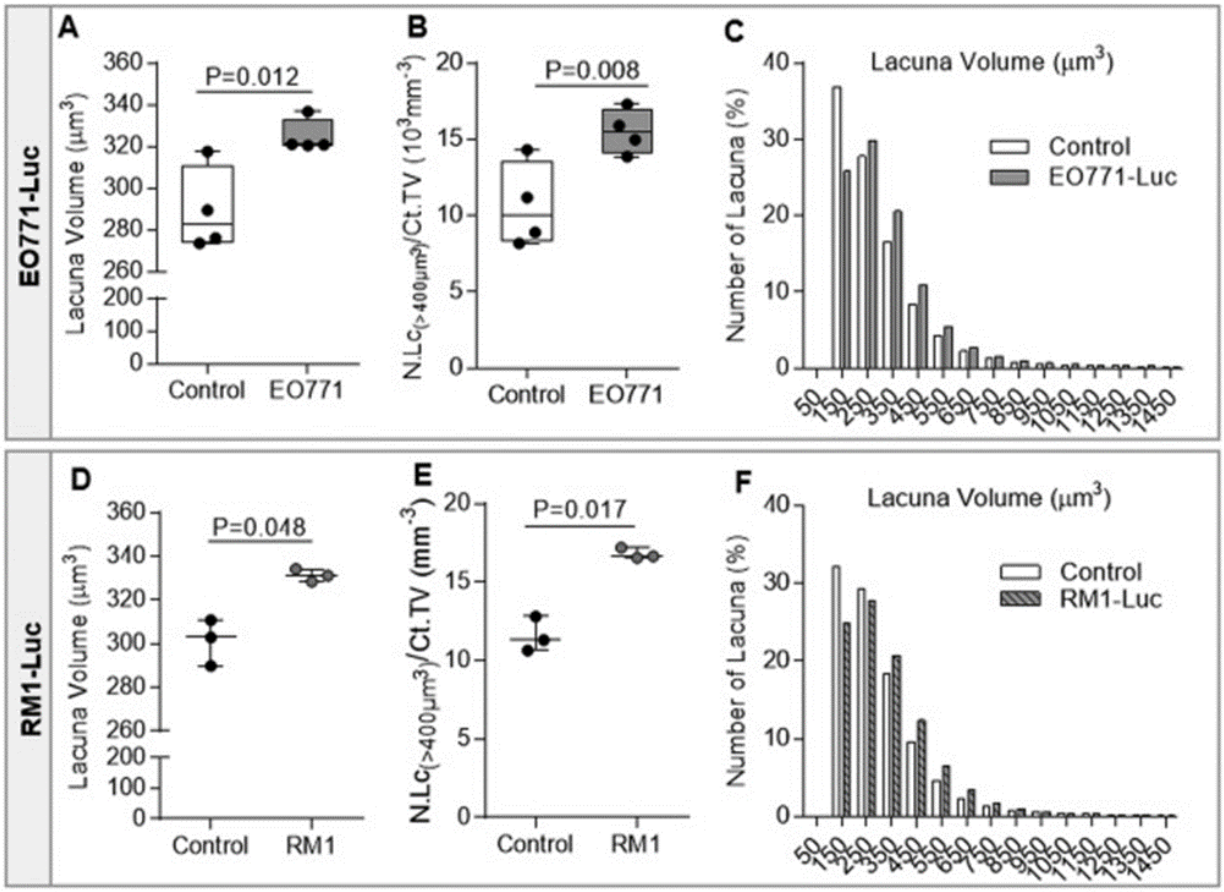

Figure 2: Micro-computed tomography evaluation reveals higher osteocyte lacuna volume after intratibial osteotropic cancer cell injection. (A,D) Mean lacuna volume of tibiae with tumour cells (EO771-Luc or RM1-Luc) in comparison to the control tibiae (PBS). (B,E) Number of large lacuna per bone volume after tumour cell injection compared to controls. (C,F) Distribution of osteocyte lacuna volume. EO771-Luc: n = 4; RM1-Luc: n = 3; paired t-tests. Image adapted by Hemmatian *et al* [27].

Regional accumulation of large lacunae with osteoblastic regions and absence of large lacunae and vascular canals near osteolytic regions (Fig.3) were identified using 3D high resolution μCT images (resolution of 0.7 μm). This result further confirmed what previously was obtained by Cui *et al* [24] and Sottnik *et al* [25]: decreased vascularization

contributes to bone loss since it may reduce the bone activity and influence the formation of osteolytic lesions. Thus, the lacuna-canalicular features of osteocytes and the blood vessel structure of cortical bone are influenced by the presence of tumour cells in the bone microenvironment.

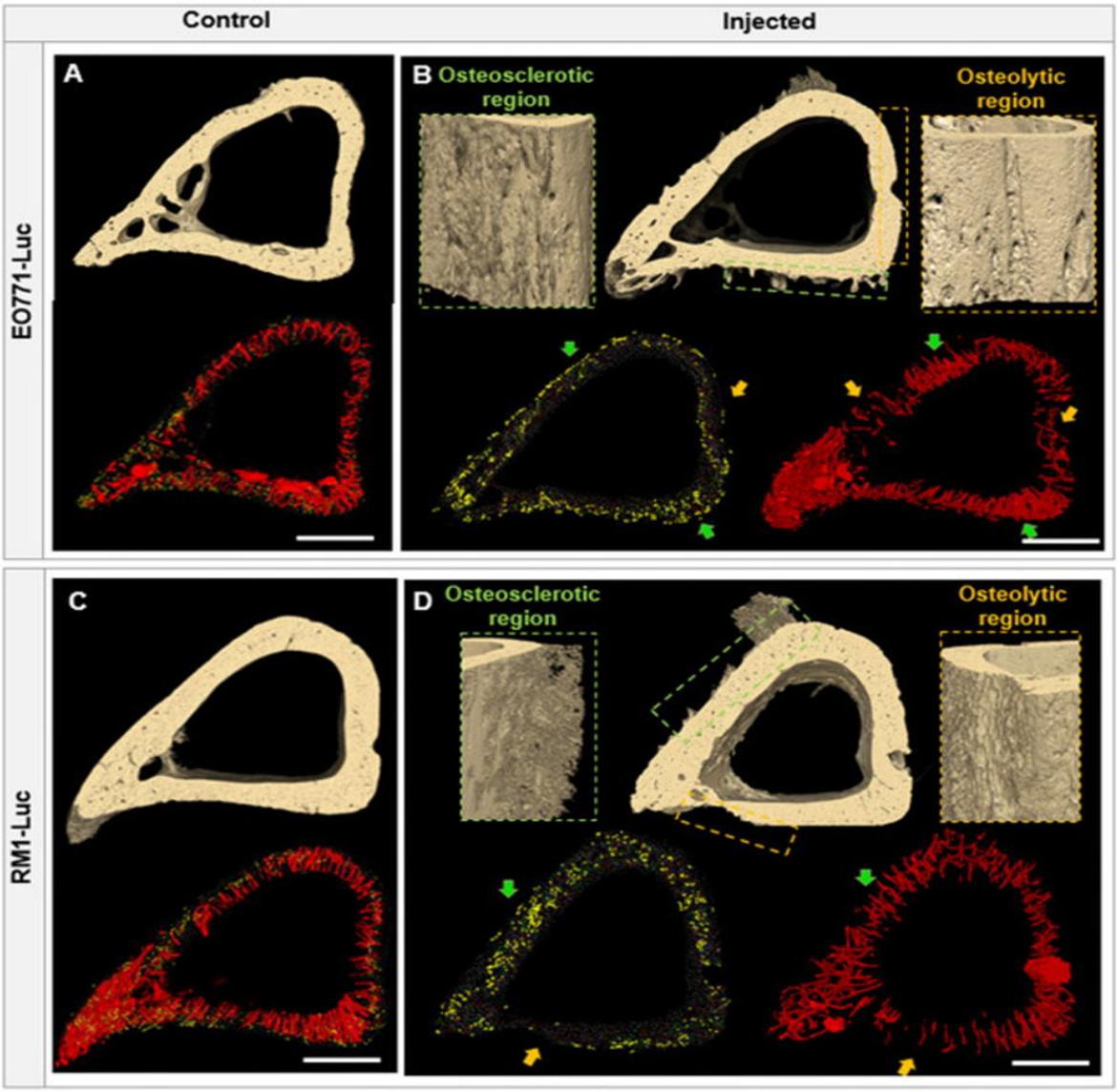

***Figure 3**:* 3D high-resolution μCT imaging of bone architecture following breast and prostate cancer cells injection identifies regional accumulation of large lacunae and vascular canals with osteosclerotic regions and absence of large lacunae and vascular canals near osteolytic regions. (A) Control sites without tumour (B) injected tibiae. The green arrows label the regions with the presence of osteosclerotic lesions, while the orange arrows indicate regions with the presence of osteolytic lesions. Scale bar = 500 μm. Image adapted by Hemmatian et al [27].

3D morphology of osteocyte lacunae can also be explored with X-ray nano-CT [26],[28]. Vatsa et al. [26], scanned calvaria and fibulae in adult mice into nano-CT (Skyscan 2011) at isotropic voxel size of 390 nm (fibula) and 480 nm (calvaria). The nano-CT images allowed to visualize the 3D morphology of osteocyte lacunae and revealed that lacunae at the two sites had different morphologies: more elongated in fibula and more spherical in calvaria. The anisotropy of osteocytes and their alignment to the local mechanical loading condition suggest that these cells can directly sense matrix strains due to external loading of bone. This reinforces the role of osteocytes as mechanosensors [15].

No osteocytes lacunae characterization on humans with metastases have been performed, but studies are focused on healthy humans. Van Hove et al. [28], measured lacunar density and the number of osteocyte lacunae in three cortical bone samples from the proximal tibia of three female patients with osteoarthritis, osteopenia, and osteopetrosis using nano-CT images (voxel size 580 nm). Matrix strains due to external loading are different in bones of different pathologies with different bone mineral density and are sensed by the osteocytes. The differences in 3D morphology of osteocytes and their lacunae in long bones of different pathologies with different mineral density might reflect an adaptation to matrix strain due to different external loading conditions. For this reason, the differences in osteocyte morphology and their lacunae indicates differences in osteocyte mechanosensitivity. These two studies support the hypothesis that osteocyte lacunar morphology depends on matrix strain.

3D osteocyte lacunar morphometric properties and distributions have also been evaluated by Dong *et al* [29] using a synchrotron X-ray micro-CT with 1.4 μm isotropic voxel resolution on thirteen human samples of femoral cortical bone. Dong *et al.* [29] decided to develop a method to get parameters at both cell and tissue levels on the same volume of interest. They calculated the number of lacunae, total and singular lacunar volume, lacunar surface area, length, width and depth of lacuna, lacunar volume density, lacunar number density and anisotropy of the bone tissue. Of the thirteen samples, the average number of lacunae was 12791, with the total lacunar volume of 0.013 mm^3, while the average and standard deviation of lacunar number density was

20,573 ± 2850/mm^3 (*N.Lc/BV*) and the lacunar volume density was 0.84% ± 0.17% (*Lc.TV/BV*).

These results are about healthy humans or animals, but there are not microstructural analyses of osteocytes lacunae in human bone with metastases. Due to the presence of osteoblastic metastases, the initial hypothesis is that the distribution and the number of osteocytes lacunae in human bone cores with metastases are different from healthy bone cores.

1.5. Aim

The aim of the study is to characterize the microstructure of osteocyte lacunae in bone cores extracted from human vertebrae with blastic metastases. In particular, the tissue mineral density, the microstructural properties of the bone and the size and position of the osteocyte lacunae will be evaluated to provide a description of the tissue at the microscale and highlight whether the spatial distribution of the lacunae could influence the formation of blastic tissue.

2. Materials and methods

2.1 Sample

This study was approved by both the Bioethics Committee of the University of Bologna (reference n. 17325, 8/02/2019) and The University of Sheffield (reference n. 031782, 22/06/2020). Three spines from donors with bone metastases with primary prostate and adrenal cancer, previously used in Palanca *et al* [30] and Cavazzoni *et al* [31], were obtained from an ethically approved donation program (Anatomy Gift Registry, AGR). Clinical CT scans (Palanca *et al* [30]) and microCT scans (Cavazzoni *et al* [31]) of the vertebrae were used to identify healthy vertebrae and vertebrae with blastic metastases.

Table 1: Donors characteristics.

Specimen ID	Donor	Age	Sex	Group	Vertebra
1	A	81	M	Blastic	L1
2	B	66	M	Blastic	L2
3	B	66	M	Blastic	L2
4	B	66	M	Blastic	L4
5	B	66	M	Blastic	L4
6	B	66	M	Blastic	L4
7	C	78	M	Blastic	L4
8	C	78	M	Blastic	L4
9	C	78	M	Blastic	L4

Nine bone cores (Table 1) were previously prepared by my supervisors at the University of Sheffield. Briefly, all the soft tissues around the vertebra were removed except for the intervertebral discs. A slice (4 mm of height) was cut from each vertebra using the EXACT

diamond band saw (EXACT Technology, USA). Then cores were extracted with the column drill (3 mm in diameter) from the 4 mm slices. Bone cores were extracted from different locations in the vertebrae from the metastatic tissue: a core in the central portion of the slice from each donor, a core in the anterior portion of the slice from donors B and C (Table 1) and a core in the lateral position of the slice from donors B and C (Table 1). Then soft tissue and bone marrow were removed from the bone cores using warm water, water jet and pliers. The epoxy resin was prepared using 10 ml of Epofix resin and 1.3 ml of Epofix hardener. Then bone cores were put into the cry-o tubes filled with the epoxy resin and then placed into a vacuum chamber. Next bone cores were put in a chemical hood to dry for at least 12 hours. At last, to expose the bone and make the two surfaces of the core parallel, a sand paper with different roughness was used, and then cores were polished using aluminum oxide.

2.2 Imaging

Each core was scanned with a high-resolution micro CT scanner (XRAdia Versa 620, Zeiss, Fig.4) at a resolution of 1.5 μm. Micro-CT is based on an X-ray tube in which the coil of the filament cathode emits X-rays: the X-ray beam passes through condenser lens that focus the X-rays on the sample [32]. The rotating anode is comprised of a tungsten-vaporized beryllium glass plate on which X-ray radiation is generated. After passing the sample, the X-rays are focused onto the detector using an objective: depending on the targeted spatial resolution, focal spot sizes between 400 and 600 nm can be selected. Projection images are acquired using the "step and shoot" technique: at a fixed focus-detector distance (FDD), the rotating platform is mounted on a base that can move in the Z-direction between the focal spot and detector [32].

The following scanning parameters were used [30]: voltage 110 kV, current 141 μA, power 15.5 W, filter LE4, pixel size 1.5 μm. These parameters enabled the scan of each core in 1.5 h. For the image reconstruction was used the standard algorithm recommended by the manufacturer.

***Figure 4**:* XRAdia Versa 620, Zeiss.

2.3 Microstructural analysis

In order to quantify microstructural parameters, a specific pipeline to post process the images was implemented.

Filtering

In order to remove the high frequency noise a gaussian blur 3D filter was applied (Fig. 5). Three different values of variance of the Gaussian filter were tested (1.5/2.5/3.5). The Gaussian blur 3D filter (variance equal to 1.5) was chosen as the best one since it permitted to eliminate frequency noise and keep all trabeculae.

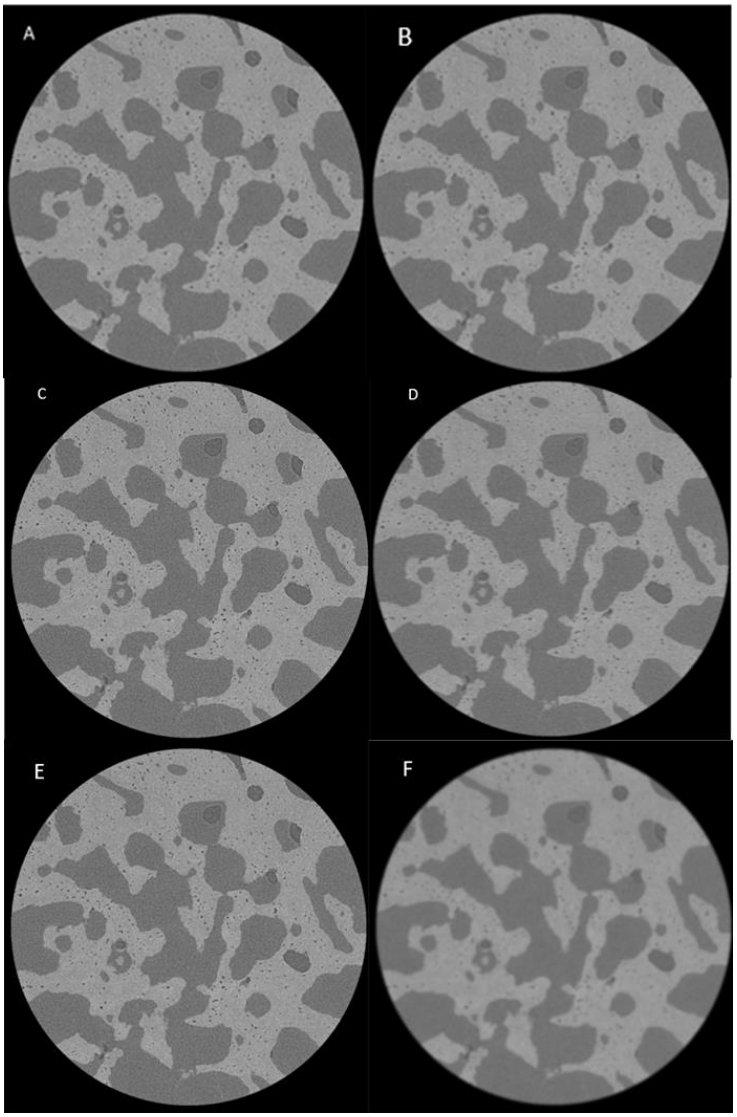

Figure 5: Comparison of three values of gaussian blur 3D filter. (A,C,E) Raw microCT image of bone core. (B) Application of Gaussian filter with variance equal to 1.5. (D) Application of Gaussian filter with variance equal to 2.5. (F) Application of Gaussian filter with variance equal to 3.5.

Thresholding

A manually selected single level threshold, calculated as the value identified by the Otsu Thresholding algorithm (ImageJ, National Institute of Health, United States) was applied to segment the images (Fig.6).

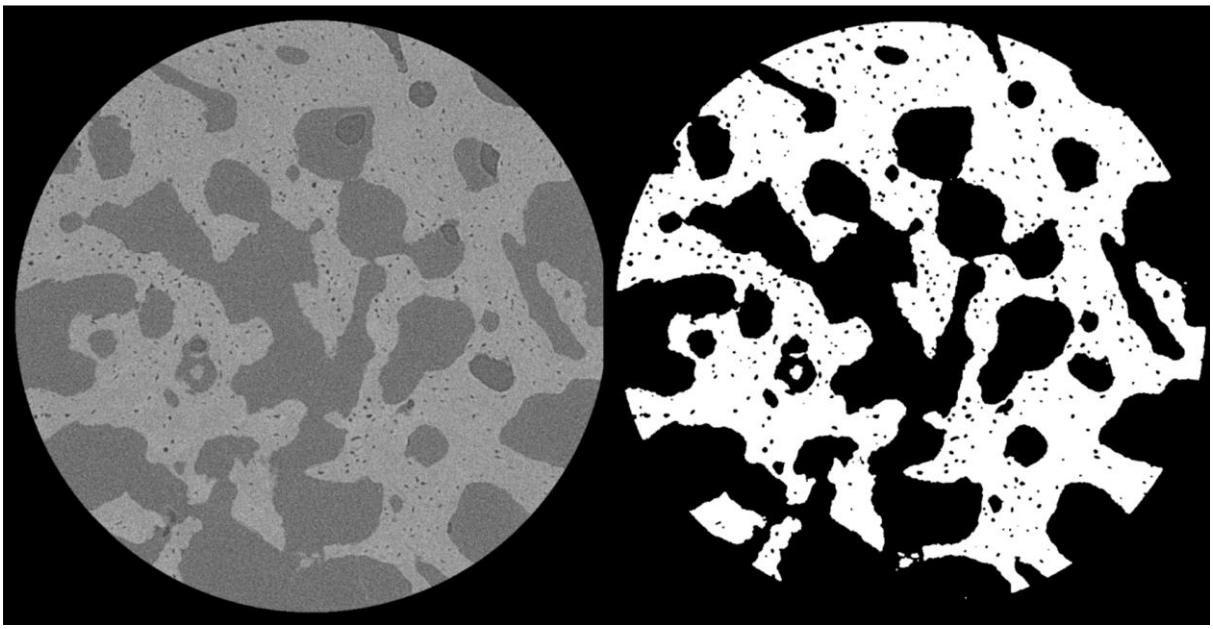

***Figure 6**:* MicroCT before (left) and after (right) the application of the threshold.

Microstructural analysis of the trabeculae (VOI_1)

The raw microCT image of bone core (Fig.7A) was used to define the main 3D microstructural parameters of the samples. In order to create binarized mask to define the Volume of interest (VOI_1) (Fig.7B) which includes all the bone cores volume, despeckling functions were applied.

The result was a binarized image with all the microporosities filled in (Fig.7C). The following 3D microstructural parameters were analysed: bone volume fraction (BV/TV_1), trabecular thickness (Tb.Th), trabecular separation (Tb.Sp) and trabecular number (Tb.N). Bone volume fraction (BV/TV_1) is defined as the proportion of the VOI occupied by binarised solid objects [33]. Trabecular thickness (Tb.Th) is defined as the mean thickness of trabeculae in the whole core. Trabecular separation (Tb.Sp) is the thickness of the spaces as defined by binarisation within the VOI [33]: Skyscan CT-analyser software measures Tb.Sp directly and model-independently in 3D by the same method used to measure trabecular thickness, just applied to the space rather than the solid voxels. Trabecular number (Tb.N) implies the number of traversals across a solid

structure, such as a bone trabecula, made per unit length through the volume of interest (VOI) [33].

Microstructural analysis of the osteocyte lacunae (VOI_2)

In order to analyse the microstructural parameters of osteocyte lacunae, a second Volume of interest was defined (VOI_2): the trabecular volume of the bone cores.

In order to create this volume, all the black speckles within 100 and 300 pixels were removed to keep only those corresponding to osteocytes lacunae. The result was a binarized image with all the osteocytes lacunae (Fig.7D). In Fig.8 the osteocytes lacunae have been highlighted in order to indicate how many are actually kept.

The following 3D microstructural parameters were analysed: total number of lacunae (N.Lc), total volume of lacunae (Lc.TV), number of lacunae density (N.Lc/TV_2), total porosity (Lc.TV/TV_2 [%]). Total number of lacunae (N.Lc) is defined as the total number of discreet binarised closed pores within the VOI: a closed pore in 3D is a connected group of space (black) voxels that is fully surrounded on all sides in 3D by solid (white) voxels [33]. Total volume of lacunae (Lc.TV) is defined as the total volume of all closed pores within the VOI [33]. Number of lacunae density (N.Lc/TV_2) is defined as the ratio between the number of lacunae and tissue volume, while total porosity (Lc.TV/TV_2 [%]) is defined as the volume of closed pores as a percent of the tissue volume.

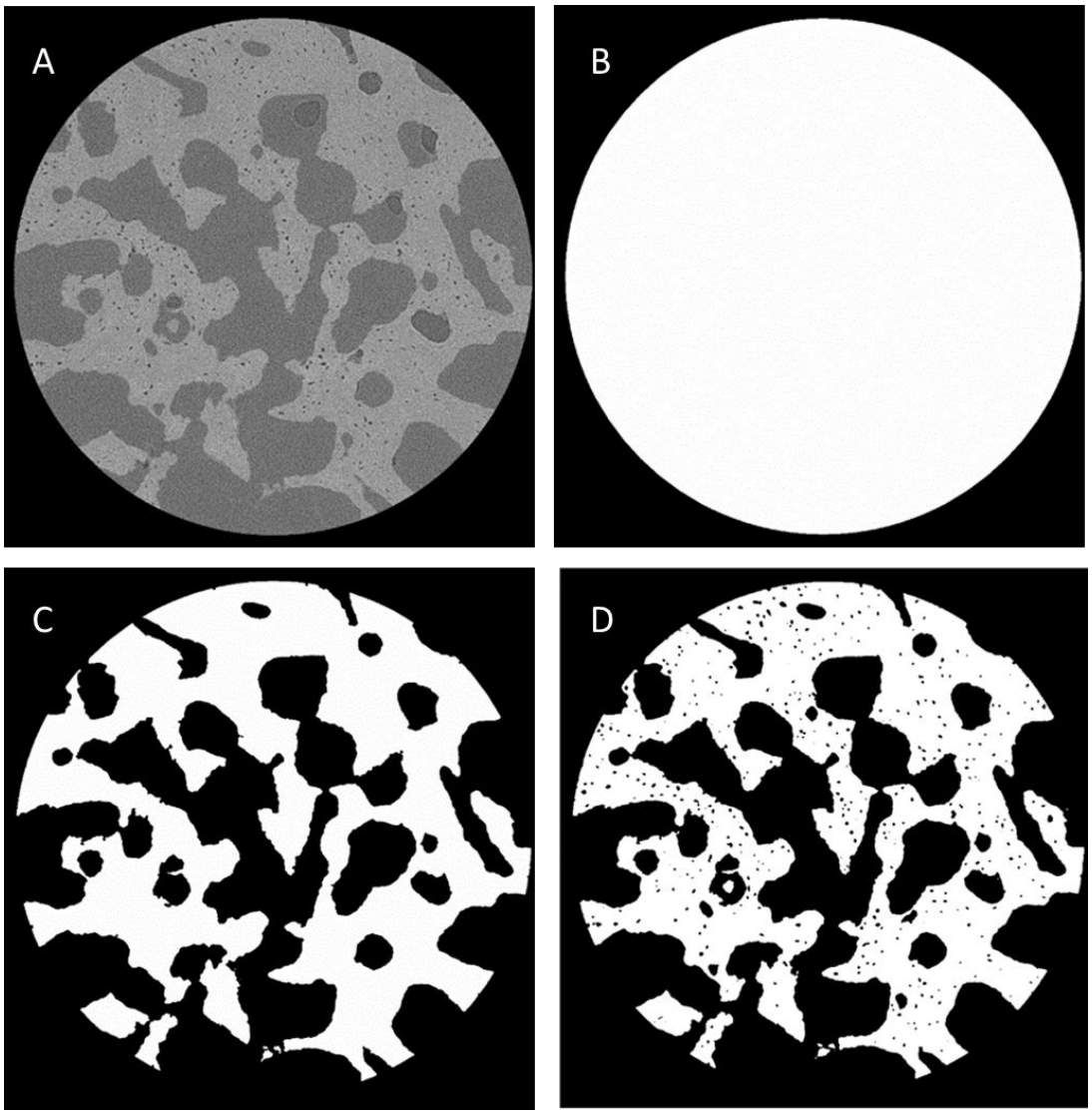

Figure 7: Process to analyse microCT images. (A) Raw microCT image of bone core. (B) VOI_1. (C) Bone cores after removing all porosities with despeckling functions. (D) Bone cores with all the osteocytes lacunae.

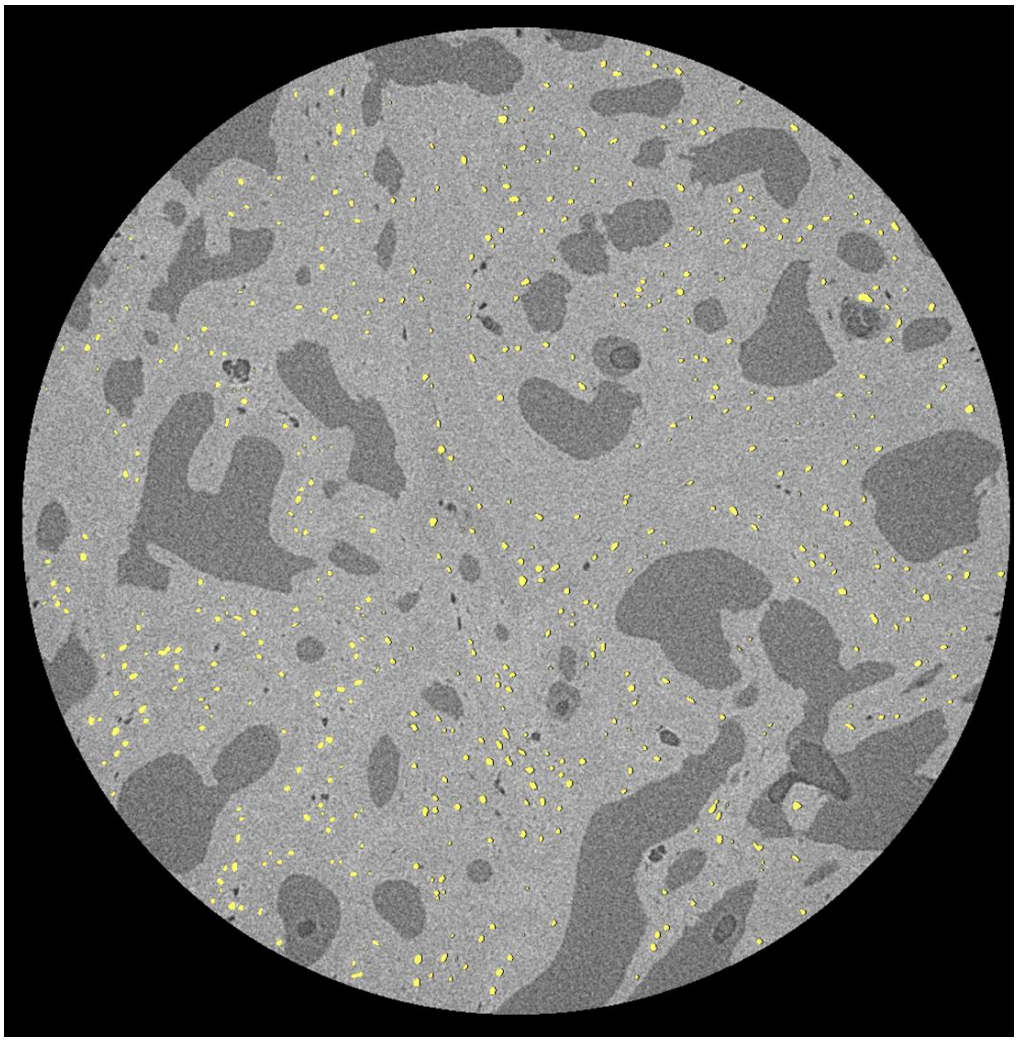

Figure 8: Osteocytes lacunae.

3. Results

3.1 Microstructural analysis of the trabeculae

After analysing the 3D microstructural parameters of the trabeculae, the mean 3D microstructural parameters were quantified among the sample (Table 2).

Table 2: 3D microstructural parameters of trabeculae.

Specimens	BV/TV_1 [%]	Tb.Th [µm]	Tb.Sp [µm]	Tb.N [mm^{-1}]	SD(Tb.Th) [µm]	SD(Tb.Sp) [µm]
1	24,53	62,28	181,14	3,94	19,10	78,76
2	51,85	113,93	153,90	4,55	45,18	79,68
3	49,49	73,74	144,47	6,71	28,91	118,74
4	70,11	141,61	93,87	4,95	60,12	52,52
5	71,30	127,37	96,57	5,60	40,13	63,97
6	55,37	123,34	123,94	4,49	67,71	59,94
7	70,91	185,11	114,75	3,83	79,43	55,65
8	71,75	244,34	169,97	2,93	99,58	96,25
9	78,16	119,87	78,18	6,52	48,55	48,68
Mean	**60,39**	**132,40**	**128,53**	**4,84**	**54,30**	**72,69**
SD	**16,85**	**55,18**	**35,97**	**1,25**	**25,24**	**23,11**

The first specimen has a lower value than the other specimens in terms of bone volume fraction (BV/TV_1): this is the only specimen extracted from the first lumbar vertebra with a primary adrenal tumor. The first and third specimens have lower values than the other specimens in terms of trabecular thickness (Tb.Th, Table 2): both these specimens were extracted from the anterior portion of the vertebrae. Furthermore, the ninth specimen has a lower value than the other specimens in terms of trabecular separation

(Tb.Sp, Table 2): this is the only specimen extracted from the central left portion of the vertebra.

3.2 Microstructural analysis of the osteocyte lacunae

After analysing the 3D microstructural parameters of the osteocyte lacunae, parameters listed in Table 3 were quantified.

Table 3: 3D microstructural parameters of osteocyte lacunae.

Specimens	N.Lc	Lc.TV [mm]	N.Lc/TV_2 [mm^{-3}]	Lc.TV/TV_2 [%]
1	17050	$9{,}48*10^{-3}$	$3{,}53*10^{4}$	1,96
2	44694	$2{,}27*10^{-2}$	$4{,}64*10^{4}$	2,36
3	27358	$5{,}50*10^{-3}$	$3{,}29*10^{4}$	0,66
4	64055	$3{,}07*10^{-2}$	$4{,}71*10^{4}$	2,26
5	74821	$2{,}35*10^{-2}$	$5{,}28*10^{4}$	1,66
6	38646	$1{,}72*10^{-2}$	$3{,}76*10^{4}$	1,67
7	53363	$1{,}86*10^{-2}$	$4{,}45*10^{4}$	1,55
8	48996	$2{,}45*10^{-2}$	$3{,}92*10^{4}$	1,96
9	63800	$2{,}68*10^{-2}$	$4{,}85*10^{4}$	2,04
Mean	**48087**	$1{,}99*10^{-2}$	$4{,}27*10^{4}$	**1,79**
SD	**18502,96**	$8{,}16*10^{-3}$	$6{,}71*10^{3}$	**0,50**

The first and third specimens have lower values than the other specimens in terms of number of lacunae (N.Lc, Table 3): both these specimens were extracted from the anterior portion of the vertebrae. Consequently, the first and third specimens have lower value than other specimens in terms of total volume of lacunae (Lc.TV, Table 3). Moreover, the

distribution of trabeculae (Fig.9) is different between the second (Fig.9A-C) and third (Fig.9D-F) donors: the third donor has a different distribution than the second donor, even though these specimens are all extracted from fourth lumbar vertebrae.

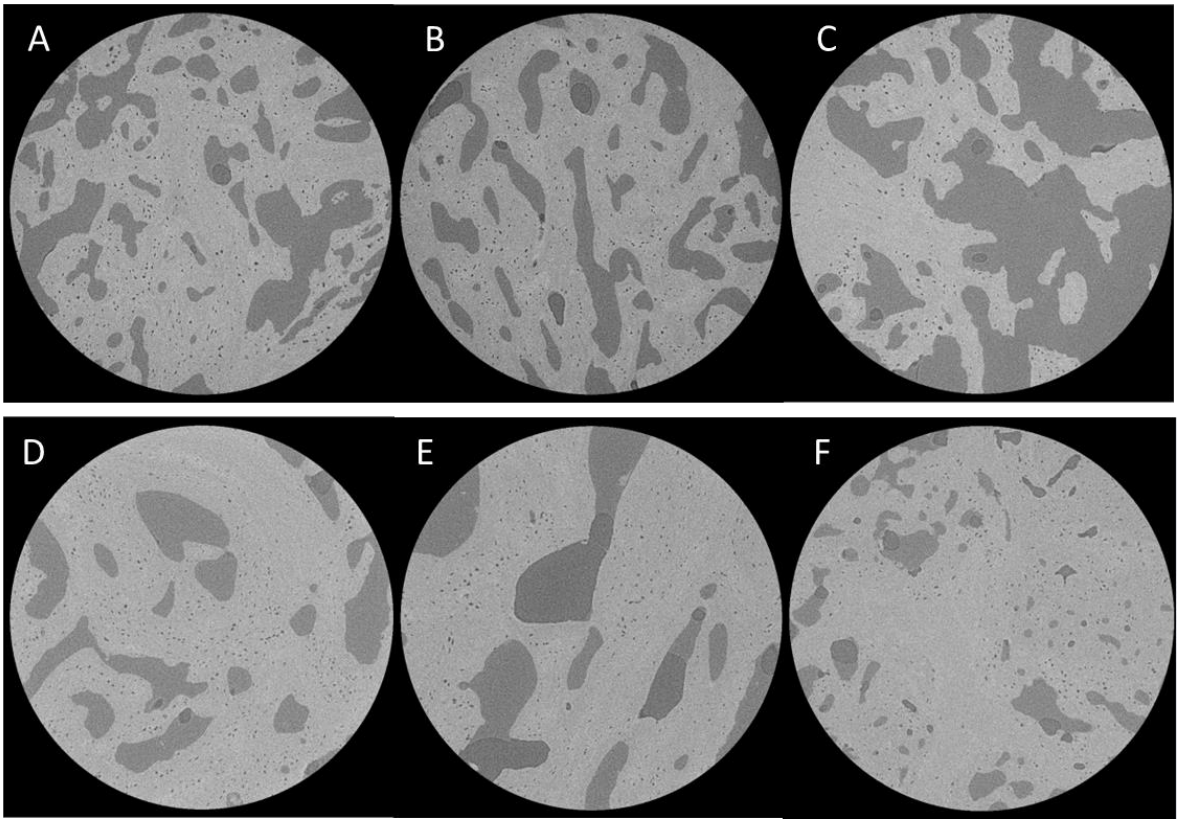

Figure 9: (A,B,C) Raw micro-CT images from the second donor. (D,E,F) Raw micro-CT images from the third donor.

4. Discussion

The aim of the study is to characterize the microstructure of osteocyte lacunae in bone cores extracted from human vertebrae with blastic metastases. In particular, the microstructural properties of the bone, the size and position of the osteocyte lacunae will be evaluated to provide a description of the tissue at the microscale and highlight whether the spatial distribution of the lacunae could influence the formation of blastic tissue.

As shown in Table 4, differences between this study and literature may be given by the fact that this study, in which bone cores are obtained from metastatic tissue are used, is

compared with papers in which cores are obtained from healthy human or animal tissue. The average value of percent bone volume (BV/TV %) obtained in our study resulted higher when compared with those of the others reference papers, as shown in Table 4, probably due to the smaller size of the specimens used in this study and the different measurement spatial resolution. The average value of trabecular thickness (Tb.Th) obtained in this study is lower compared to the one obtained from the second lumbar vertebra by Hasegawa [36], but similar to the results obtained by Kusins [35] and Wei [37]. The average value of trabecular separation (Tb.Sp) of this study is lower compared to the results in the literature. These result are probably due to the fact that this study and the ones by Kusins [35] and Wei [37] have been performed on bone cores, while Hasegawa [36] used the whole lumbar vertebra. Furthermore, the mean value of trabecular separation (Tb.Sp) in this study is lower than other studies because tumors are caused by uncontrolled proliferation of cells, such as osteoblasts, which form new bone tissue: this situation creates new trabecular tissue, causing the reduction of trabecular separation (Tb.Sp).

Table 4: Comparison between the values of 3D microstructural parameters of trabeculae in this study and Kusins [35], Hasegawa [36] and Wei [37].

References	Imaging tech	Location	Voxel size [µm]	Sample number	BV/TV [%]	Tb. Th [μm]	Tb. Sp [μm]	Tb. N [mm^{-1}]
This study	Nano CT	Vertebral cores	1.5	9	60,39 ± 16,85	123,40 ± 55,18	128,53 ± 35,97	4,84 ± 1,25
Kusins et al, 2021	Micro CT	Human humeral head–neck junction cores	4.75	10	16,1	140	750	1,11
Hasegawa et al, 2023	Micro CT	Human vertebra (L2)	50	1	9,47 ± 1,24	267,6 ± 8,2	996,1 ± 95,1	0,286 ± 0,032
Wei et al, 2022	Micro CT	Pig femurs	9	6	36 ± 7	130 ± 20	-	2,69 ± 0,45

The average value of the number of lacunae in the whole specimen (N.Lc) in this study resulted to be higher when compared to the human femoral mid-diaphysis cores (Dong et al [29]) as shown in Table 5: this is probably due to the fact that in Dong *et al* [29] the characterization is made only on cortical bone, while in Goff *et al* [39] the number of lacunae (N.Lc) is similar to this study since it considered both cortical and trabecular regions. Furthermore, this is probably related to the fact that this study used cores extracted from blastic tissue while other papers used healthy bones. Moreover, the average value of the total volume of lacunae (Lc.TV) in this study resulted to be higher when compared to Goff *et al* [39] even though the number of lacunae resulted to be similar. For those reasons, the average value of the number density of lacunae (N.Lc/TV) in this study

resulted to be higher compared to the others papers in which bone cores are extracted from healthy human bones (Dong et al [29] , Goff et al [39]). Since osteocytes control mechanosensation and mechanotransduction in bones, an higher value of the number desnsity of lacunae (N.Lc/TV) could indicate an high bone formation by osteoblasts, which during bone formation remain trapped in the bone matrix becoming osteocytes. This study, in fact, used bone cores extracted from vertebrae with blastic tissue, while the other studies used healthy human bones: tumours are characterized by the uncontrolled proliferation of cells, such as osteoblasts, so these results indicate that in these cores metastases could develop more.

***Table 5**: C*omparison between the value of 3D microstructural parameters of osteocytes lacunae in this study and Dong [29], Britz [38] and Goff [39].

References	Imaging tech	Location	Voxel size [µm]	Sample number	N.Lc	Lc.TV [mm^3]	N.Lc/TV [mm^{-3}]	Lc.TV/TV (%)
This study	Nano CT	Vertebral cores	1,5	9	48087 ± 18503	0,0199 ± 0,0082	$4{,}27*10^4$ ± $6{,}71*10^3$	1,79 ± 0,50
Dong et al, 2014	SR µCT	Human femoral mid-diaphysis cores	1,47	13	12791 ± 2531	0,0052 ± 0,0013	$2{,}0*10^4$ ± $2{,}85*10^3$	0,84 ± 0,17
Britz et al, 2012	SR µCT	Rat tibia diaphysis	2	6	-	-	$6{,}3 * 10^4$ ± $1{,}96 * 10^3$	-
Goff et al, 2021	Ultra-high resolution micro-CT	Transiliac human bone	1,2	31	41200	0,0063	$2{,}6 *10^3$	0,04

For what concern spatial distribution of the lacunae, in micro-CT images is possible to highlight the presence of areas with a high density of osteocyte lacunae alternating with areas with a low density or without any osteocytes (Fig.9). Osteocytes are formed from osteoblasts which, during the deposition of bone tissue, remain trapped in the bone matrix: area with high density of osteocyte lacunae may indicate high bone formation by osteoblasts. Since tumours are characterized by the uncontrolled proliferation of cells, such as osteoblasts, these areas with high density of osteocyte lacunae could be areas in which metastases can develop.

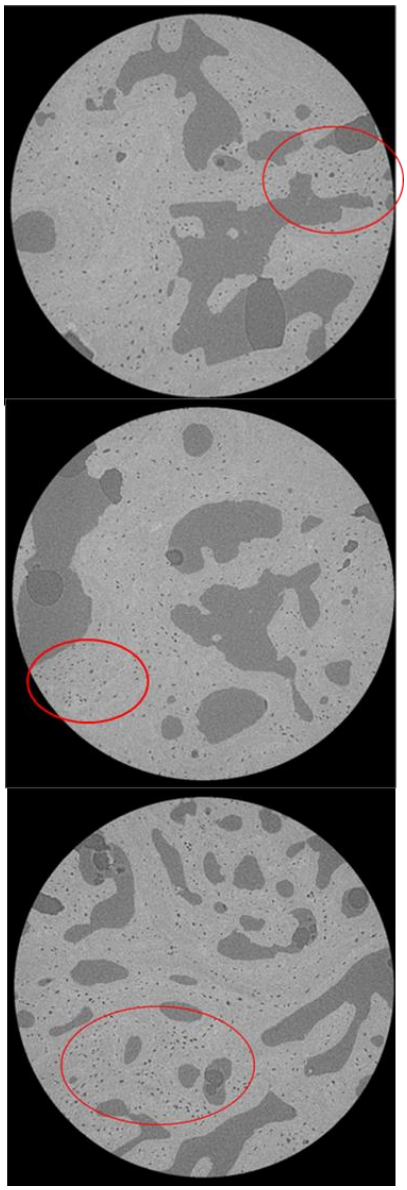

***Figure 9**:* Areas with high density of osteocyte lacunae.

4.1 Limitations of the study

This study has few limitations. The first one is the sample size: nine specimens were obtained from three donors. A larger sample size, both in terms of specimens and donors, should be tested to confirm the preliminary findings observed in this study.

Due to the small number of specimens, it was not possible to perform a robust statistical analysis. Thus, a descriptive statistic was reported to compare the 3D parameters of the different specimens.

Moreover, since in this study the mean values of the microstructural parameters of the bone cores extracted from vertebrae with blastic tissue were evaluated, it was not possible to carry out a quantitative analysis of the spatial distribution of osteocytes lacunae but only a qualitative one through the nano-CT scans. In fact, in this study it is not possible to determine the value of this parameter in each region of the cores.

It was not possible to compare the obtained values of the microstructural parameters with those of healthy bone cores from the same donors. Values have been only compared with some scientific studies concerning the characterization of the bone microstructural parameters of healthy humans or animals with bone metastases. A larger sample size, in terms of specimens from healthy and metastatic donors should be tested to confirm the preliminary findings observed in this study.

5. Conclusions

In this study a microstructural analysis was performed on nine bone cores extracted from human vertebrae with blastic metastases previously scanned with clinical CT and micro-CT. The aim of the study is to characterize the microstructure of osteocyte lacunae in bone cores extracted from human vertebrae with blastic metastases. In particular, the microstructural properties of the bone, the size and position of the osteocyte lacunae will be evaluated to provide a description of the tissue at the microscale and highlight whether the spatial distribution of the lacunae could influence the formation of blastic tissue.

This was the first study performed on bone cores extracted from blastic metastases localized in human vertebrae. It has been possible to compare the results obtained with other studies from the literature performed on healthy human bones or bones from animals with metastases induced. The outcomes showed differences in both trabecular and osteocytes lacunae parameters between this study and the literature. Indeed, both trabecular thickness (Tb.Th) and trabecular separation (Tb.Sp) resulted to be lower in this study when compared to literature: this is in line with the fact that this study used bone cores with metastatic tissue, while other papers used whole healthy human bones or animals with metastases. In fact, tumors are caused by uncontrolled proliferation of cells, such as osteoblasts, which form new bone tissue: this situation creates new trabecular tissue, causing the reduction of trabecular separation (Tb.Sp). For what concern microstructural analysis of osteocytes lacunae, the number of lacunae (N.Lc) resulted to be lower in this study when compared to studies based on cortical bone cores. On the other hand, the total volume of lacunae (Lc.TV) and the density number of lacunae (N.Lc/TV) resulted to be higher in this study compared to other studies. Since osteocytes control mechanosensation and mechanotransduction in bones, an higher value of the number desnsity of lacunae (N.Lc/TV) could indicate an high bone formation by osteoblasts, which during bone formation remain trapped in the bone matrix becoming osteocytes. Moreover, the total volume of lacunae in this study is higher than other papers with similar values of number of lacunae. For what concern spatial distribution of the osteocyte lacunae, from micro-CT images it is possible to highlight the presence of areas with a high density of osteocyte lacunae alternating with areas with a low density or without any osteocytes. Since tumours are characterized by the uncontrolled proliferation of cells, such as osteoblasts, from which osteocytes are formed, these areas with high density of osteocyte lacunae could be areas in which metastases can develop more.

In conclusion, the outcomes of this study highlight the importance of investigating microstructural parameters of osteocytes lacunae in bone cores extracted from vertebrae with blastic tissue to understand their role in the formation and development of blastic tissue.

Ringraziamenti

Voglio innanzitutto ringraziare i miei relatori Marco Palanca, Giulia Cavazzoni e Enrico dall'Ara per avermi dato la possibilità di partecipare a questo importante progetto e avermi dato la fiducia e le conoscenze necessarie per svolgerlo al meglio. Sono contenta di aver potuto fare un'esperienza di questo tipo sin dalla triennale poiché certamente mi ha dato strumenti che nel mio futuro mi torneranno utili.

Per chi mi conosce sa che non sono tipo da parole sentimentali, ma farò questo sforzo solo per voi.

Ringrazio i miei genitori per avermi dato la possibilità di studiare, ma soprattutto di avermi sempre sostenuto in ogni momento importante della mia vita.

Ringrazio i miei fratelli, Simone e Franco, per esserci sempre stati per me, sia nei momenti belli ma anche nei momenti più brutti: dopotutto una sorellina avrà sempre bisogno dei suoi fratelloni. In particolare, voglio ringraziare Simone, per avermi sempre sostenuto durante i miei studi, in particolare universitari: hai sempre creduto in me ciecamente, indipendentemente dal risultato finale.

Voglio poi ringraziare Riccardo: il mio fan numero uno in tutto e per tutto. Probabilmente tre quarti delle cose belle che sono riuscita a fare in questi anni è anche grazie a te. Mi spingi sempre a buttarmi nelle cose, a dare il meglio di me, alle volte rompendo anche, ma senza di te con chi potrei lamentarmi ogni giorno, ma soprattutto, a chi potrei rompere le scatole h24?

Ringrazio le mie ame, le bros, compagne di vita: anche voi sapete bene che il mio linguaggio dell'amore non è né fisico e né tantomeno parole, ma sapete che vi voglio un mondo di bene. Ci siete sempre state per ogni cosa e spero che rimarrete qui a sopportarmi per tanto altro tempo.

Infine, ringrazio tutti quelli che sono potuti venire qui in questo giorno importante per me: Elisa, Beatrice, Stefania, i miei nonni.

Infine, vorrei mandare un pensiero anche alla mia Zia Paola: sei stata molto importante nella mia vita e sono sicura che saresti felicissima di vedermi qui con questa corona. Tutto questo è anche grazie a te.

6. References

[1] Patricia A Downey e Michael I Siegel, «Bone Biology and the Clinical Implications for Osteoporosis», 2006. [Online]. Disponibile su: https://doi.org/10.1093/ptj/86.1.77

[2] E. Bilgiç, Ö. Boyacıoğlu, M. Gizer, P. Korkusuz, e F. Korkusuz, «Chapter 6 - Architecture of bone tissue and its adaptation to pathological conditions», in *Comparative Kinesiology of the Human Body*, S. Angin e I. E. Şimşek, A c. di, Academic Press, 2020, pp. 71–90. doi: 10.1016/B978-0-12-812162-7.00006-0.

[3] Alizae Marny Mohamed, «An Overview of Bone Cells and their Regulating Factors of Differentiation», Mohamed AM. An overview of bone cells and their regulating factors of differentiation. Malays J Med Sci. 2008 Jan;15(1):4-12. PMID: 22589609; PMCID: PMC3341892., 2008.

[4] R. Florencio-Silva, G. R. da S. Sasso, E. Sasso-Cerri, M. J. Simões, e P. S. Cerri, «Biology of Bone Tissue: Structure, Function, and Factors That Influence Bone Cells», *BioMed Research International*, vol. 2015, p. 421746, lug. 2015, doi: 10.1155/2015/421746.

[5] F. G. F. Tresguerres, J. Torres, J. López-Quiles, G. Hernández, J. A. Vega, e I. F. Tresguerres, «The osteocyte: A multifunctional cell within the bone», *Annals of Anatomy - Anatomischer Anzeiger*, vol. 227, p. 151422, gen. 2020, doi: 10.1016/j.aanat.2019.151422.

[6] Lei Qin, Wen Liu, Huiling Cao,corresponding author and Guozhi Xiao, «Molecular mechanosensors in osteocytes». [Online]. Disponibile su: https://www.ncbi.nlm.nih.gov/pmc/articles/PMC7280204/

[7] I. P. Selestin Raja *et al.*, «Polyphenols-loaded electrospun nanofibers in bone tissue engineering and regeneration», *Biomaterials Research*, vol. 25, set. 2021, doi: 10.1186/s40824-021-00229-3.

[8] «Histology at SIU». [Online]. Disponibile su: https://histology.siu.edu/ssb/remodel.htm

[9] DIMITRIOS J. HADJIDAKIS,IOANNIS I. ANDROULAKIS, «Bone Remodeling». [Online]. Disponibile su: https://doi-org.ezproxy.unibo.it/10.1196/annals.1365.035

[10] E. F. Eriksen, «Cellular mechanisms of bone remodeling», *Reviews in Endocrine and Metabolic Disorders*, vol. 11, fasc. 4, pp. 219–227, dic. 2010, doi: 10.1007/s11154-010-9153-1.

[11] Y. G. Yuan Jianmin; Zhang, Lingli; Tong, Xiaoyang; Zhang, Shihua; Zhou, Xuchang; Zhang, Miao; Chen, Xi; Lei, Le; Li, Hui; Liu, Timon Cheng Yi; Xu, Jiake; Zou, Jun, «MiR-214 Attenuates the Osteogenic Effects of Mechanical Loading on Osteoblasts», *Int J Sports Med*, vol. 40, fasc. 14, pp. 931–940, dic. 2019, doi: 10.1055/a-1015-0285.

[12] L. F. Bonewald e M. L. Johnson, «Osteocytes, mechanosensing and Wnt signaling», *Bone*, vol. 42, fasc. 4, pp. 606–615, apr. 2008, doi: 10.1016/j.bone.2007.12.224.

[13] Y. Han, S. C. Cowin, M. B. Schaffler, e S. Weinbaum, «Mechanotransduction and strain amplification in osteocyte cell processes», *Proceedings of the National Academy of Sciences*, vol. 101, fasc. 47, pp. 16689–16694, nov. 2004, doi: 10.1073/pnas.0407429101.

[14] L. H. Xu, H. Shao, Y.-H. V. Ma, e L. You, «OCY454 Osteocytes as an in Vitro Cell Model for Bone Remodeling Under Mechanical Loading», *Journal of Orthopaedic Research*, vol. 37, fasc. 8, pp. 1681–1689, ago. 2019, doi: 10.1002/jor.24302.

[15] Coughlin, T. R., Romero-Moreno, R., Mason, D. E., Nystrom, L., Boerckel, J. D., Niebur, G., & Littlepage, L. E., «(2017). Bone: A Fertile Soil for Cancer Metastasis. Current drug targets, 18(11), 1281–1295.», 2017.

[16] G. R. Mundy, «Mechanisms of bone metastasis», *Cancer*, vol. 80, fasc. S8, pp. 1546–1556, ott. 1997, doi: 10.1002/(SICI)1097-0142(19971015)80:8+<1546::AID-CNCR4>3.0.CO;2-I.

[17] R. Coleman, «Incidence and distribution of bone metastases», presentato al Metastatic Bone Disease: Fundamental and Clinical Aspects, Springer, 1994, pp. 20–30.

[18] G. D. Roodman, «Mechanisms of Bone Metastasis», *N Engl J Med*, vol. 350, fasc. 16, pp. 1655–1664, apr. 2004, doi: 10.1056/NEJMra030831.

[19] G. Maccauro, M. S. Spinelli, S. Mauro, C. Perisano, C. Graci, e M. A. Rosa, «Physiopathology of Spine Metastasis», *International Journal of Surgical Oncology*, vol. 2011, p. 107969, ago. 2011, doi: 10.1155/2011/107969.

[20] S. Bailey, D. Hackney, D. Vashishth, e R. N. Alkalay, «The effects of metastatic lesion on the structural determinants of bone: Current clinical and experimental approaches», *Bone*, vol. 138, p. 115159, set. 2020, doi: 10.1016/j.bone.2019.115159.

[21] M. H. ISLER e R. E. TURCOTTE, «CHAPTER 29 - Bone Tumors in Children», in *Pediatric Bone*, F. H. GLORIEUX, J. M. PETTIFOR, e H. JÜPPNER, A c. di, San Diego: Academic Press, 2003, pp. 703–743. doi: 10.1016/B978-012286551-0/50031-2.

[22] Karaguzel, G., & Holick, M. F., «Diagnosis and treatment of osteopenia.», 2010. [Online]. Disponibile su: https://doi.org/10.1007/s11154-010-9154-0

[23] Turner, J., Parsi, M., & Badireddy, M., «Anemia», 2022.

[24] «New Roles of Osteocytes in Proliferation, Migration and Invasion of Breast and Prostate Cancer Cells». [Online]. Disponibile su: https://ar.iiarjournals.org/content/36/3/1193.long

[25] J. L. Sottnik, J. Dai, H. Zhang, B. Campbell, e E. T. Keller, «Tumor-Induced Pressure in the Bone Microenvironment Causes Osteocytes to Promote the Growth of Prostate Cancer Bone Metastases», *Cancer Research*, vol. 75, fasc. 11, pp. 2151–2158, mag. 2015, doi: 10.1158/0008-5472.CAN-14-2493.

[26] A. Vatsa, R. G. Breuls, C. M. Semeins, P. L. Salmon, T. H. Smit, e J. Klein-Nulend, «Osteocyte morphology in fibula and calvaria — Is there a role for mechanosensing?», *Bone*, vol. 43, fasc. 3, pp. 452–458, set. 2008, doi: 10.1016/j.bone.2008.01.030.

[27] H. Hemmatian *et al.*, «Reorganization of the osteocyte lacuno-canalicular network characteristics in tumor sites of an immunocompetent murine model of osteotropic cancers», *Bone*, vol. 152, p. 116074, nov. 2021, doi: 10.1016/j.bone.2021.116074.

[28] «Van Hove, R. P., Nolte, P. A., Vatsa, A., Semeins, C. M., Salmon, P. L., Smit, T. H., & Klein-Nulend, J. (2009). Osteocyte morphology in human tibiae of different bone pathologies with different bone mineral density--is there a role for

mechanosensing?. Bone, 45(2), 321–329. https://doi-org.ezproxy.unibo.it/10.1016/j.bone.2009.04.238».

[29] P. Dong *et al.*, «3D osteocyte lacunar morphometric properties and distributions in human femoral cortical bone using synchrotron radiation micro-CT images», *Bone*, vol. 60, pp. 172–185, mar. 2014, doi: 10.1016/j.bone.2013.12.008.

[30] M. Palanca *et al.*, «Type, size, and position of metastatic lesions explain the deformation of the vertebrae under complex loading conditions», *Bone*, vol. 151, p. 116028, ott. 2021, doi: 10.1016/j.bone.2021.116028.

[31] G. Cavazzoni, L. Cristofolini, E. Dall'Ara, e M. Palanca, «Bone metastases do not affect the measurement uncertainties of a global digital volume correlation algorithm», *Frontiers in Bioengineering and Biotechnology*, vol. 11, 2023, doi: 10.3389/fbioe.2023.1152358.

[32] M. ; L. Kampschulte A. C. ;. Sender, J. ;. Litzlbauer, H. D. ;. Althöhn, U. ;. Schwab, J. D. ;. Alejandre-Lafont, E. ;. Martels, G. ;. Krombach, G. A., «Nano-Computed Tomography: Technique and Applications», *Rofo*, vol. 188, fasc. 02, pp. 146–154, gen. 2016, doi: 10.1055/s-0041-106541.

[33] A. M. Parfitt *et al.*, «Bone histomorphometry: standardization of nomenclature, symbols, and units: report of the ASBMR Histomorphometry Nomenclature Committee», *Journal of bone and mineral research*, vol. 2, fasc. 6, pp. 595–610, 1987.

[34] «Hildebrand T and Ruegsegger P (1997a) A new method for the model independent assessment of thickness in three dimensional images. J. Microsc. 185: 67-75.»

[35] J. Kusins, N. Knowles, N. Martensson, M. Columbus, G. Athwal, e L. Ferreira, «Full-Field Experimental Analysis of the Influence of Microstructural Parameters on the Mechanical Properties of Humeral Head Trabecular Bone», *Journal of Orthopaedic Research*, vol. 40, dic. 2021, doi: 10.1002/jor.25242.

[36] H. Hasegawa, N. Nango, e M. Machida, «Evaluation of Trabecular Microstructure of Cancellous Bone Using Quarter-Detector Computed Tomography», *Diagnostics*, vol. 13, fasc. 7, 2023, doi: 10.3390/diagnostics13071240.

[37] W. Wei, F. Shi, e J. F. Kolb, «Analysis of microstructural parameters of trabecular bone based on electrical impedance spectroscopy and deep neural networks», *Bioelectrochemistry*, vol. 148, p. 108232, 2022, doi: https://doi.org/10.1016/j.bioelechem.2022.108232.

[38] H. M. Britz *et al.*, «Prolonged unloading in growing rats reduces cortical osteocyte lacunar density and volume in the distal tibia», *Bone*, vol. 51, fasc. 5, pp. 913–919, 2012, doi: https://doi.org/10.1016/j.bone.2012.08.112.

[39] E. Goff *et al.*, «Large-scale quantification of human osteocyte lacunar morphological biomarkers as assessed by ultra-high-resolution desktop micro-computed tomography», *Bone*, vol. 152, p. 116094, 2021, doi: https://doi.org/10.1016/j.bone.2021.116094.